Journal of Inorganic Biochemistry 194 (2019) 52–64

Contents lists available at ScienceDirect

Journal of Inorganic Biochemistry

journal homepage: www.elsevier.com/locate/jinorgbio

Anticancer activity and mechanism of bis-pyrimidine based dimetallic Ru(II) (η^6-*p*-cymene) complex in human non-small cell lung cancer *via* p53-dependent pathway

Muhammad Zeeshan Bhatti[a,b], Amjad Ali[a,c], Hong-Quan Duong[d], Jiwu Chen[e,*], Faiz-Ur Rahman[f,g,**]

[a] Shanghai Key Laboratory of Regulatory Biology, Institute of Biomedical Sciences, School of Life Sciences, East China Normal University, Shanghai 200241, China
[b] Department of Biological Sciences, National University of Medical Sciences, Rawalpindi 46000, Pakistan
[c] Institute of Integrative Biosciences, CECOS University of IT and Emerging Sciences, Peshawar, KPK, Pakistan
[d] Institute of Research and Development, Duy Tan University, K7/25 Quang Trung, Danang 550000, Viet Nam
[e] School of Life Sciences, East China Normal University, Shanghai 200241, China
[f] Center for Supramolecular Chemistry and Catalysis, Department of Chemistry, Shanghai University, Shanghai 200444, China
[g] Department of Chemistry, Fudan University, 2005 Songhu Road, Shanghai 200438, China

ARTICLE INFO

Keywords:
Anticancer complex
p53 activation
Cell migration
bis-Pyrimidine ligand
Ru-cymene

ABSTRACT

Non-small cell lung cancer (NSCLC) is the most common cancer worldwide, which is related with poor prognosis and resistance to chemotherapy. Notably, ruthenium-based complexes have emerged as good alternative to the currently used platinum-based drugs for cancer therapy. In the present study, we synthesized a novel bis-pyrimidine based ligand 1,3-bis(2-methyl-6-(pyridin-2-yl)pyrimidin-4-yl)benzene (L) and used it in the synthesis of a dimetallic Ru(II) cymene complex [$(Ru(\eta^6$-*p*-cymene)Cl$)_2$(1,3-bis(2-methyl-6-(pyridin-2-yl)pyrimidin-4-yl) benzene)] (L-Ru). We checked the stability of this complex in solution state in D_2O/DMSO-d_6 mixture and found it to be highly stable under these conditions. We determined the anticancer activity and mechanism of action of L-Ru in human NSCLC A549 and A427 by 3-(4,5-dimethylthiazol-2-yl)-2,5-diphenyltetrazolium bromide (MTT) and related biological analyses. These results revealed that L-Ru exerted a strong inhibitory effect on the cells proliferation,G0/G1-arrest, accompanied with upregulation of p53, p21, p15, cleaved Poly (ADP-ribose) polymerase (PARP) protein and downregulation of cell cycle markers. L-Ru inhibited cell migration and invasion. The mitochondria-mediated apoptosis of NSCLC induced by L-Ru was also observed followed by the increase of apoptosis regulator B-cell lymphoma 2 associated X (BAX), and activation of caspase-3/-9. The effects of L-Ru on the cell viability, Terminal deoxynucleotidyl transferase dUTP nick end labeling (TUNEL) positive cells and Annexin V-positive cells apoptosis induction were remarkably attenuated. This complex induced DNA damage, cell cycle arrest and cell death *via* caspase-dependent apoptosis involving PARP activation and induction of p53-dependent pathway. These findings suggested that this ruthenium complex might be a potential effective chemotherapeutic agent in NSCLC therapy.

1. Introduction

Cancer is one of the leading causes for health problem, with significant associated death and disabilities worldwide [1]. Treatment against cancer can have some difficulties in molecular level because the tumor cells are able to change all the genetic defense mechanism and repair of the DNA molecule form the activation of proto-oncogenes and inactivation of suppressor genes, including several DNA-repair pathways as well as DNA-damage [2]. In the past decade, lung cancer is one of the most frequently diagnosed cancers and has the highest mortality rate worldwide [3], making it the second-most frequent cause of cancer-related death in males and females [4,5]. Non-small cell lung cancer (NSCLC) is found in approximately 80% of all lung cancer cases. Amplification of oncogenes, activation of survival signaling and genomic instability play key role in the progression of NCSLC and thus promote resistance against chemotherapeutic agents. There are several

* Corresponding author.
** Correspondence to: F. U. Rahman, Center for Supramolecular Chemistry and Catalysis, Department of Chemistry, Shanghai University, Shanghai 200444, China.
E-mail addresses: jwchen@bio.ecnu.edu.cn (J. Chen), faizurrahman@fudan.edu.cn (F.-U. Rahman).

https://doi.org/10.1016/j.jinorgbio.2019.01.019
Received 4 October 2018; Received in revised form 17 January 2019; Accepted 17 January 2019
Available online 23 February 2019
0162-0134/

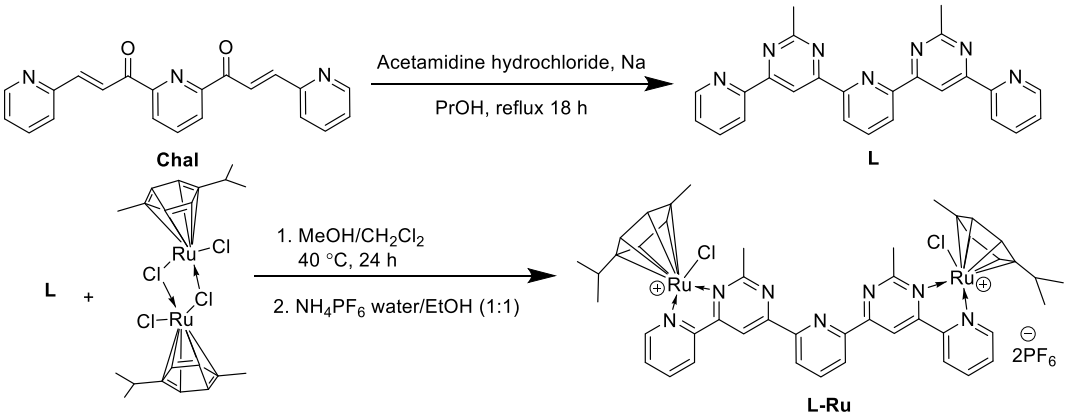

Scheme 1. Synthesis scheme for L and L-Ru.

therapeutic approaches to the treatment of lung cancer, including chemotherapy [4,6]. Currently, radiotherapy and chemotherapy are still the standard therapy method, but only a modest increase in survival rate is found after the application of radio-therapy and chemotherapy [7]. Thus, the development of effective therapeutic agents is important and urgent for lung cancer treatment.

Over the past decades, a variety of metal complexes have been identified in the anticancer therapy [8,9]. Cisplatin (CP; *cis*-diamminedichloroplatinum II), a first–line chemotherapeutic agent based on damaging the DNA structure and/or its function, has long been used to suppress a number of different solid tumors, including head and neck, bladder, testicular, cervical, ovary, breast, esophageal and NSCLC [1,10,11]. Although cisplatin is a high cytotoxic drug, but still resistance is common due to several genetic and epigenetic changes in cancer cells [4,12,13]. The drug acts primarily as a DNA-damaging agent through interaction with purine bases in DNA and formation of DNA-DNA and DNA-protein inter and intrastrand crosslinks, including growth arrest and/or apoptosis [14,15]. The mechanism of cisplatin-induced anticancer therapy is widely through to be interrelated with DNA synthesis and replication, and considered as mainstay in anticancer chemotherapy. However, serious side effects on the normal body tissues/organ such as ototoxicity, genetic toxicity, myelosuppression, neurotoxicity, and allergic reactions, and intrinsic or acquired resistance to cisplatin are the major therapeutic problems for cancer chemotherapy, which have limited its applications [15,16].

Thus, an increasing number of investigations have been carried out on the safer and effective chemoprevention and development is required for the improvement of the efficiency and lower the treatment cost of chemotherapy [1,17]. At present, much attention has focused on ruthenium compounds since they displayed significant antitumor activity, low toxicity to normal tissues, no cross-resistance with cisplatin, and easy absorption by tumor micro-environment [18,19]. Ruthenium complexes have emerged as part of new approaches to cancer therapy and have showed extremely promising results in the development of novel metal anticancer drugs, the studies on their action mechanisms have attracted wide attention in the past years [20–24]. Many researchers have discovered that DNA and some intercellular proteins are main targets of Ru complexes [25–27]. Polypyridyl Ru(II) compounds can induce cancer cell apoptosis by targeting mitochondria and causing the overproduction of reactive oxygen species [28,29]. The *cis*-$[RuCl_2(NH_3)_4]Cl$ complex presented cytotoxicity, reduction of tumor growth and increased survival time of animals on murine sarcoma (S180) using *in-vitro* and *in-vivo* assays [30]. Several studies reported that ruthenium (III) and (II) complexes exhibited a potent antitumor activity *in-vitro* by inducing apoptotic mechanism [31,32], and induction of DNA damage [31,33]. Ruthenium II complexes induce cell death against murine Sarcoma (S180) *via* induction of apoptosis [17,34–36]. To the date, many researches are focused on the interaction between ruthenium complexes and intercellular biomacromolecules. However, till now little information on the mechanism of apoptosis by ruthenium complexes is available. It remains unclear that how ruthenium complexes triggers apoptosis in cancer cells.

Our research group is working on metal complexes against anticancer activity in different kinds of cancer cell lines [16,37–41]. Therefore, in this paper we synthesized a new dimetallic Ru(II) cymene complex [(Ru(η^6-*p*-cymene)Cl)2(1,3-bis(2-methyl-6-(pyridin-2-yl)pyrimidin-4-yl)benzene)] (L-Ru) appended on a bis-pyrimidine based ligand 1,3-bis(2-methyl-6-(pyridin-2-yl)pyrimidin-4-yl)benzene (L) in excellent yield and characterized by detailed analytical methods. This complex was found to be highly stable in solution state as revealed by repeated ^{1}H NMR analysis over three days. The cytotoxicity assays against NSCLC A549 and A427 cell lines were carried out using 3-(4,5-dimethylthiazol-2-yl)-2,5-diphenyltetrazolium bromide (MTT) method. In addition, we analyzed the effect of this complex on cell morphology and cell migration as well as mechanism of cell death induced and changes in cell cycle arrest. Furthermore, the ability of this ruthenium complex to promote apoptosis was investigated by apoptotic gene regulation and activation of caspase-3/-9.

2. Results

2.1. Chemical synthesis

bis-Pyrimidine based ligand L was synthesized in goog yield by base catalyzed cyclization of chalcone (Chal) with acetamidine hydrochloride in refluxing ethanol. 1 equivalents L was reacted with 1.1 equivalents of dichloro(*p*-cymene)ruthenium(II) dimer in methanol/dichloromethane mixture during 24 h (Scheme 1). Pure solid of the complex (L-Ru) was isolated in excellent yield from the reaction mixture dissolved in ethanol by anions exchange from chloride to hexafluorophosphate. It was characterized by IR, ^{1}H, ^{13}C NMR spectroscopy and HR-MS (ESI) spectrometry and elemental analysis.

2.2. Stability of L-Ru

The stability of an anticancer agent is crucial especially when it is a metal-based compound. As metal easily coordinate with a number of solvents and affected by air, light *etc.*, therefore it is important to check the stability in solid as well as in solution state. Several previous studies showed the influence of stability on the anticancer activities of a particular complex. Different techniques like NMR and UV spectroscopy, MS, LC-MS or GC–MS spectrometry analyses were used for the stability study of different Ru or other metal complexes in solution state [42–45]. Similarly, fast aquation was observed for several Ru-cymene based complexes [42]. We found L-Ru to be stable in solid state under air and light, as we performed ^{1}H NMR analysis for the same sample we

prepared 20 months before (ESI Fig. S1). Similarly, we performed ^{1}H NMR analysis for L-Ru over three days in 20% D_2O/DMSO-d_6 (ESI Fig. S2). The repeated ^{1}H NMR analyses over three days showed no change in the proton chemical shifts or numbers. These results showed this complex resist aquation and it is highly stable under these laboratory conditions (presence of DMSO and water).

However, Ru complexes aquation of the ancillary chloride ligand is an important phenomenon and it facilitates their interaction with biomolecules. This aquation also decreases the stability of these compounds and they become more susceptible to break down or interaction with other biomolecules instead reaching the target. Similarly, their proper clinical administration may also be difficult and become problematic for proper evaluation. Therefore, different modification could stabilize the labile nature of the chloride ligand, at least to achieve the stability in laboratory conditions [46].

We achieved this stability in L-Ru, and showed this complex is stable in water/DMSO under laboratory conditions. Inside cancer cell conditions are different therefore we can assume that aquation of chloride ligand occurred and the aquated complex interacted with the target biomolecule and resulted in apoptosis of the cells. Similarly, the loss of arene function to make active specie or other non-covalent interaction of L-Ru with biomolecule could not be omitted and they may also be responsible for effective cancer cells apoptosis. But all these processes are hard to monitor inside cancer cells and may require further detailed analyses.

2.3. Inhibition of cell proliferation

In order to evaluate the cytotoxic activity of the ruthenium complex (L-Ru), the *in-vitro* assays were carried out against NSCLC A549 and A427 cell lines. Cisplatin was used for comparison, under identical conditions. In this assay, these compounds were incubated with cells for 24 h. As shown in Fig. 2A, the cytotoxic effect of L-Ru (0–20 μM) and positive control CP (0–20 μM (an established chemotherapeutic agent) were assessed to optimum concentrations for the prevention of tumor growth on A549 and A427 cells. As a result, significant change was observed in the cell viability of L-Ru treated A549 and A427 cells at higher concentration of L-Ru (20 μM) with respect to control (untreated) (Fig. 1A). Based on these results, further analysis was carried out at concentration of 20 μM as a most significant concentration.

Next we performed colony formation assay to determine the cell proliferation of L-Ru and CP (20 μM) treated A549 and A427 cells. The results demonstrated that 20 μM concentration of L-Ru was the most effective, and that cell proliferation inhibition was drastically reduced as compare to control group in A549 and A427 cells (Fig. 2B, C). These results indicated that L-Ru treatment inhibited cell proliferation and colony formation of NSCLC cells.

2.4. Morphological analysis of cells by AO/EB and Hoechst 33342 staining

Cell death through apoptosis is essential for anticancer activity of complexes. Apoptosis was investigated with staining method utilizing acridine orange (AO) and ethidium bromide (EB) under fluorescence microscope. The AO/EB staining is sensitive to DNA and was used to assess changes in the nuclear morphology. Control cells (live and healthy) produce bright green fluorescence with normal cytoplasm and nuclei morphology. Whereas, A549 and A427 cells treated with L-Ru display yellowish green fluorescence with membrane bleeding containing apoptotic bodies and red necrotic cells represented apoptosis (Fig. 2A). These characteristic features are typical of apoptotic cells and are very different from cells shown in control. Furthermore, the nuclear morphological changes during apoptosis after 24 h of drugs treatment, fluorescence staining was done with DNA binding dye Hoechst-33342 followed by microscopy technique to analyze the morphological feathers of nuclei to discriminate apoptotic, necrotic, and viable cells. In control cells, normal nuclei with uniform blue chromatin were observed which indicated healthy cells with no nuclear disruption. Whereas, L-Ru-induced cellular death was indicated by cell with bright colored, nuclear shrinking, chromatin condensed and cytoplasmic bleeding in A549 and A427 cells were observed in comparison with CP as a positive control (Fig. 2B). These results indicated that exposure of L-Ru has ability to triggers the apoptotic pathway of cells death in NSCLC cell lines.

2.5. Induction of cell apoptosis by L-Ru

To determine the ability of L-Ru to induce A549 and A427 cells apoptosis was analyzed by annexin fluorescein isothiocyanate/propidium di-iodide staining (FACS/PI). The results showed that the number of apoptotic cells in the L-Ru and CP group was significantly higher than that in the control group (Fig. 3A). Compared with control, cellular apoptosis in the L-Ru was significantly higher in A549 and A427 cells, respectively (Fig. 3B). To further validate the apoptosis induced by L-Ru in A549 and A427 cells, Terminal deoxynucleotidyl transferase (TdT) dUTP nick-end labeling (TUNEL) assay was performed to detect the presence of any DNA stand breaks, as well known hallmark of apoptosis. After exposed with L-Ru and CP (positive control), cells showed significant increase in TUNEL positive cells as compared to the negative control cells in A549 and A427 cells (Fig. 3C and D). This data indicated that L-Ru greatly induced cells apoptosis compared with control group. However, L-Ru induced evident apoptosis almost similar to CP in both cancer cell lines.

2.6. Cell cycle inhibition

Next we investigated whether L-Ru complex can suppress DNA synthesis by blocking cell cycle progression. The cell cycle distribution of A549 and A427 cells, after 24 h of incubation with 20 μM of L-Ru and CP (positive control) was performed using flow cytometric analysis. According to flow cytometry histogram data, treatment of A549 and A427 cells with complexes induces shift in the population of cells during cell cycle as compared to negative control. 20 μM concentration of L-Ru led to an increase in the percentage of cell in G0/G1 cell cycle phase by 15.72% and G0/G1 phase by 16.42% in A549 and A427 cells, respectively (Fig. 4A). However, graphical representation of L-Ru showed 10–12% lower G0/G1 arrest comparing with of CP in A549 and A427 cells, respectively (Fig. 4B). These results indicate that L-Ru has ability to reduce DNA synthesis by inhibiting S and G2/M phase.

2.7. L-Ru activates caspase-3/-9 cascade

Next we asked whether L-Ru has the ability to activate caspase-dependent signaling in NSCLC cells. Caspase-dependent signaling plays an important role in the activation of apoptosis. Interestingly, we observed caspase-3 activity was significantly increased with L-Ru treatment in both cells, whereas cells exposed to CP exhibited more dramatic activation of caspase-3 (Fig. 5A). Taken together, these results indicated that compared to CP, the apoptotic effect of ruthenium induced in NSCLC cells involved caspase-3 activation at an earlier period. To further understand the potential mechanism of ruthenium induced apoptosis, the initiator of the intrinsic and intrinsic pathways activator caspase-9 was investigated. The results showed that treatment with 20 μM of L-Ru for 24 h significantly increased the activity of caspase-9 (Fig. 5B). Caspase activation play critical role in proteolytic cleavage of cleaved Poly (ADP-ribose) polymerase (PARP), which is regarded as a biochemical marker of cells undergoing apoptosis [47]. Treatment with L-Ru significantly activated the cleavage of PARP in both cancer cells lines (Fig. 5C). The results suggested that L-Ru effectively triggered the activation of the extrinsic and intrinsic apoptosis pathways, and the mitochondria-mediated pathways may have an important effect on cell apoptosis.

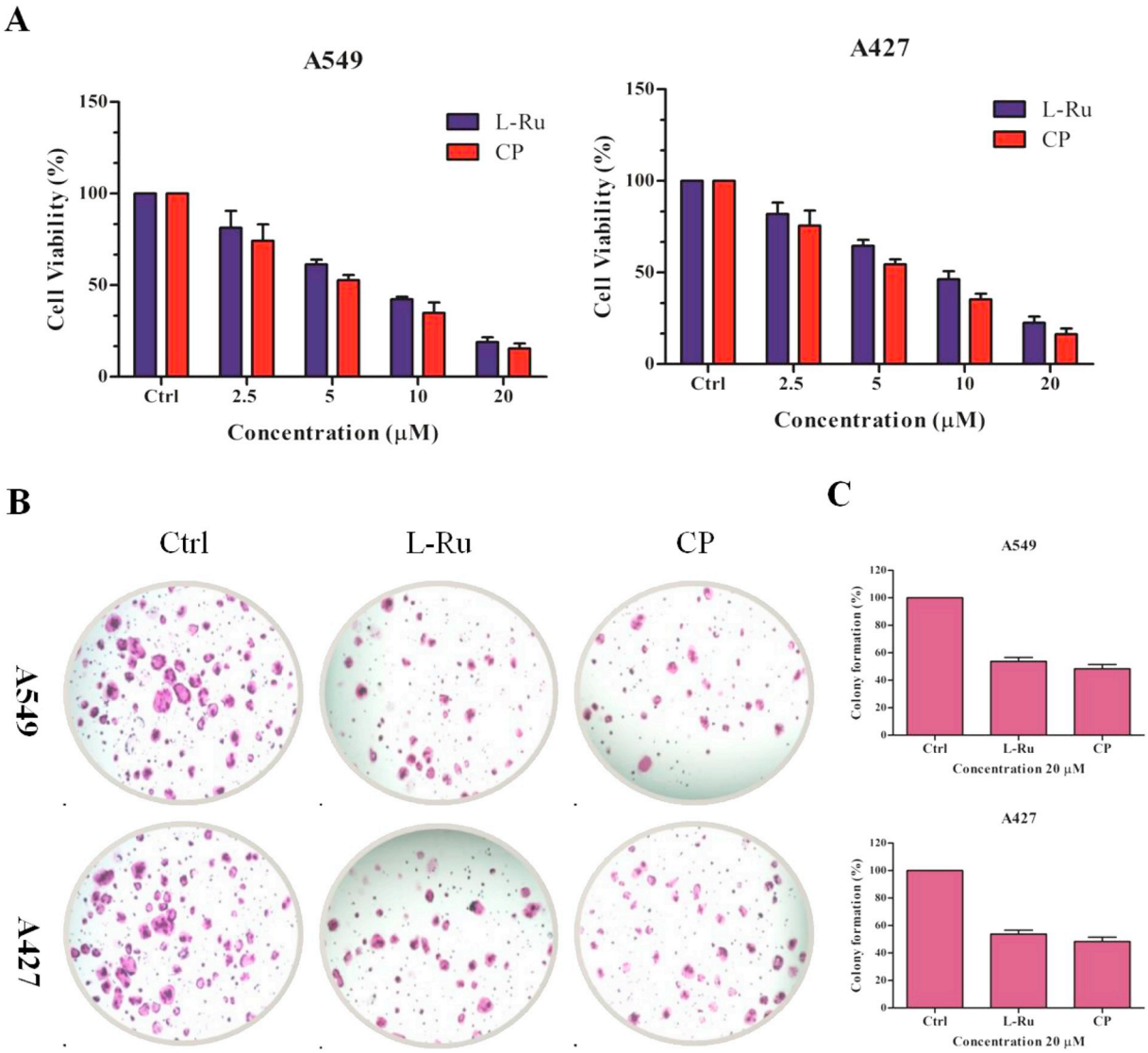

Fig. 1. Inhibition of cell proliferation by ruthenium complex. (A) MTT assay to determine cell viability of L-Ru treated A549 and A427 cells, after 24 h of incubation with 0–20 μM concentration. (B) Represented images of colony formation assay in A549 and A427 cells, after exposure with 20 μM of L-Ru and CP as a positive control. (C) Analyzed in percentage inhibition of cologenic ability in A549 and A427 cells.

2.8. Effect of L-Ru on the expression of apoptosis and cell cycle associated proteins

Next we investigated the underlying molecular mechanism that how L-Ru complex induces apoptosis and suppresses cell cycle progression. We found that the treatment of A549 and A427 cells with L-Ru significantly enhanced p53, p21, p15 tumor suppressor proteins expressions. In contrast, cell treated with L-Ru showed inhibition of c-Myc (myelocytomatosis) oncogene expression coupled with suppression of cell cycle regulatory proteins such as cyclin D1, cyclin A1, and cyclin B1 (Fig. 6A). In sum, these results indicate that L-Ru has ability to regulate thee subset of protein expressions that play important role in apoptosis, cancer progression and cell cycle regulation.

2.9. Effect of L-Ru on the mRNA expression level of p53 target genes

Tumor suppressor p53 mainly act as a transcription factor and has ability to control the expression of several target genes that play important role in cell proliferation, migration and cell cycle progression. Therefore, qRT-PCR (quantitative real-time polymerase chain reaction) analysis was performed to determine the expression profile of p53 downstream and upstream target genes in NSCLC cells. Results showed that L-Ru affected the expression of apoptosis regulator Bax (B-cell lymphoma 2 associated X), PUMA (p53 upregulated modulator of apoptosis), and NoxA (Phorbol-12-myristate-13-acetate-induced protein 1) genes and increased the mRNA expression levels in A549 cells. Similarly, A427 indicated higher mRNA expression of Bax, PUMA, and NoxA genes compared with control cells. The most pronounced effect of L-Ru was noted on Bcl2 (B-cell lymphoma 2) mRNA expression in treated cells. The exposure of L-Ru to A549 cells resulting decreased in Bcl-2 and hTERT (Telomerase reverse transcriptase) transcript levels, whereas decreased in Bcl-2 and NoxA in A427 cells was obtained (Fig. 6B). These magnitude of changes in p53 target genes expression in treated cells indicated towards apoptotic induction properties of complexes in NSCLC cells.

2.10. L-Ru complex inhibits migration and invasion

Cell migration and invasion play role in cancer metastasis. Blocking of cell invasion has been linked with suppression of cancer progression. To address the role of ruthenium in the regulation of migration and invasion in NSCLC cells, transwell assays were performed. The results

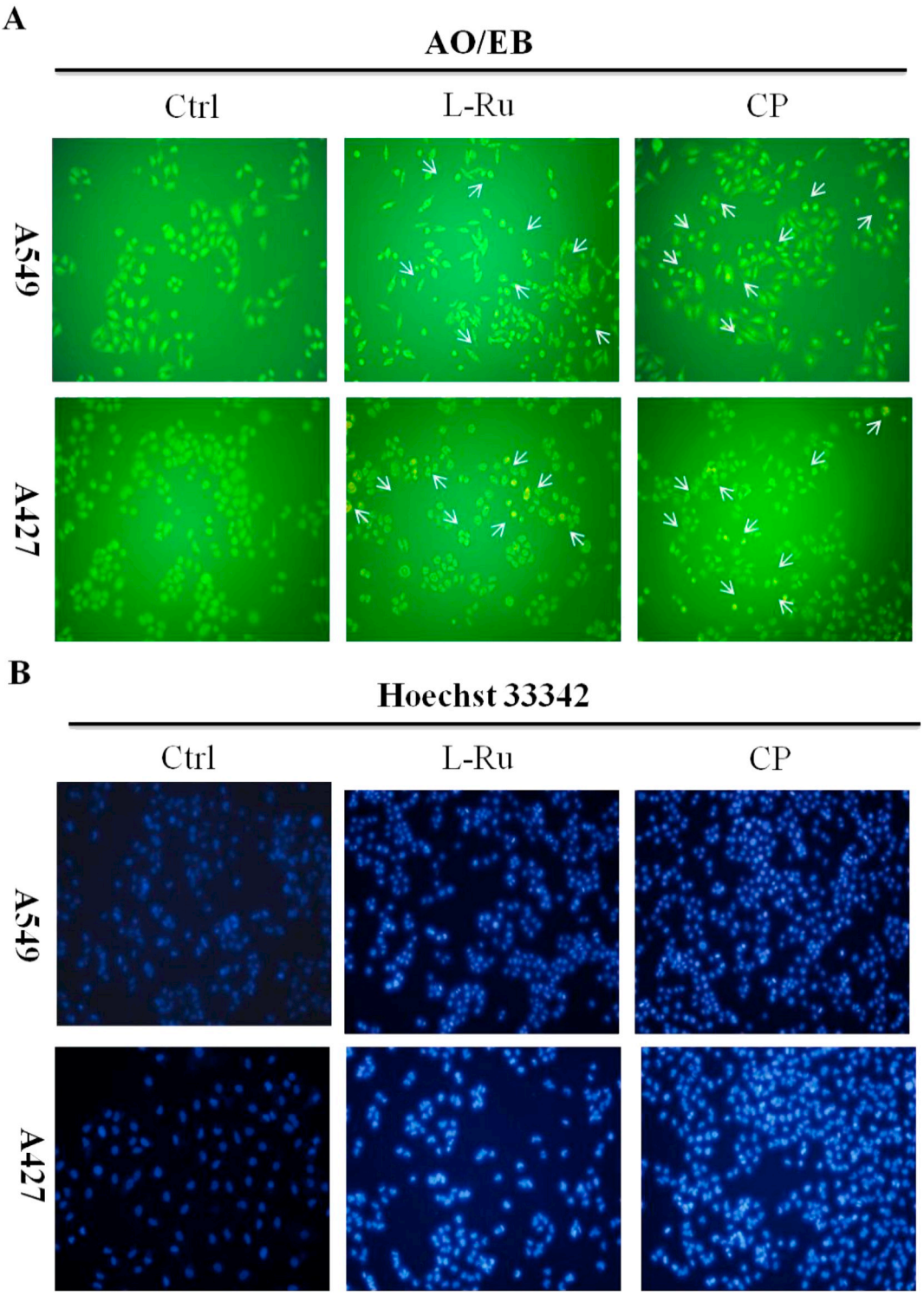

Fig. 2. Effect of L-Ru on NSCLC cells morphology apoptosis. (A) A549 and A427 cells were stained with AO/EB and observed under fluorescence microscopy. In the presence of L-Ru (20 μM) incubated for 24 h. Cells showed living cell in green, arrows indicate apoptotic and necrotic cells exhibit orange or red color, respectively. (B) Hoechst-33342 staining after 24 h of L-Ru and cisplatin treatment was visualized under the fluorescence microscope (magnification 20×).

showed that L-Ru treated cells significantly suppressed the migration of A549 and A427cells (Fig. 7A, B). Similarly, the invasion ability of A549 and A427 cells were also reduced by L-Ru treatment (Fig. 7C, D). The migration and invasion capacity was compared with standard drug CP as a positive control in both assays. These data suggested that L-Ru treatment suppresses migratory and invasive abilities of NSCLC cells.

3. Discussions

Human cancer is a complex and highly diverse disease based on multiple etiologies, multiple cell targets and distinct developmental stages. Cancer development involves several genetic and epigenetic changes. One of the major hallmarks of cancer is the resistance of cancer cells against chemotherapy. Imitation of apoptosis signaling play crucial role in the elimination of cancer cells by cell death mechanism.

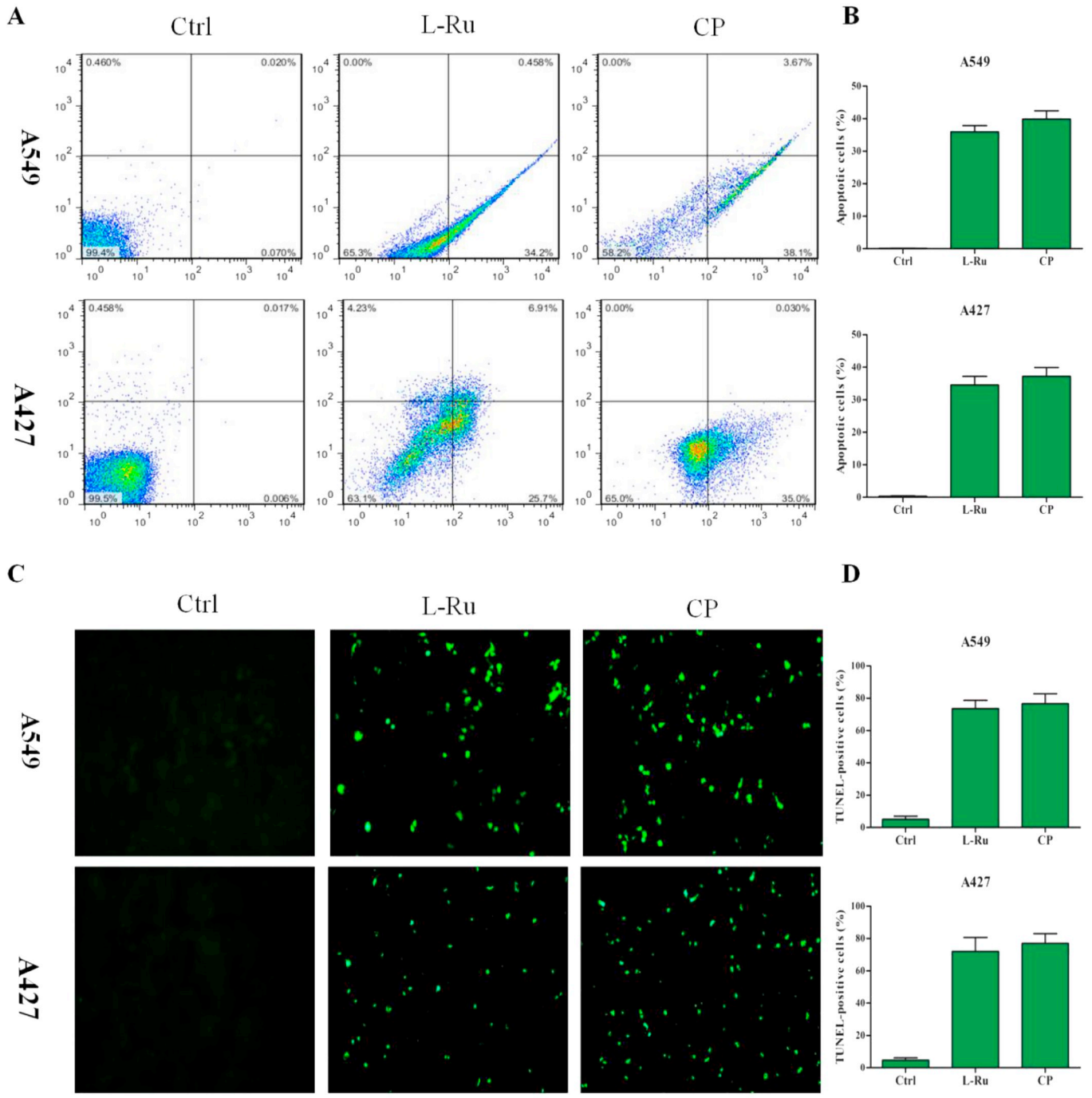

Fig. 3. Effects of apoptosis on NSCLC by L-Ru. (A) Flow cytometric analysis of L-Ru inducing cell death by double staining test. A549 and A427 cells were treated with 20 μM of L-Ru for 24 h. Positive control contain CP treatment with same concentration of L-Ru for 24 h. (B) Represent percentage analysis of Annexin V-FITC/PI analysis in A549 and A427 cells. (C) A549 and A427 cells were analyzed by TUNEL assay, after incubation with 20 μM of L-Ru for 24 h. Representative images (20 ×) of TUNEL assay were obtained by fluorescence microscopy. (D) Right panel represent percentage analysis of TUNEL assay in A549 and A427 cells. Values represent mean ± SD of three independent experiments.

A key process in the ability to tumor cells to expand locally is resistance to apoptosis. The suppression of apoptotic potential can involve the activation of anti-apoptosis factors [48]. The programmed cell death or apoptosis mechanism plays a critical role in various physiological processes, such as maintenance of homeostasis during the development of adult tissue and control immunologic activity. The dys-regulation of apoptosis pathways, one of the hallmarks of cancer cells, has been found in several diseases including cancer [49]. Previously, it was found that *cis*-[RuCl(BzCN)(bipy)(dppe)]PF_6 (BzCN = benzonitrile, bipy = 2,2′-bipyridine, dppe = 1,2-bis(diphenylphosphino) ethane) complex was cytotoxic against murine leukemia (S180), prostate (DU-145), leukemia (K572), and lung (A549) cells with IC_{50} values 17.0, 7.16, 11.6, and 20.0 μM, respectively [50]. In this study, we demonstrated that L-Ru exhibit higher and preferential cytotoxicity against NSCLC A549 and A427 cells. Our results demonstrated that that L-Ru exhibited higher efficacies in killing NSCLC cells. However, L-Ru showed modest cytotoxic potential and apoptosis activity in association with CP. To confirm these results, clonogenic cell survival assay determines the ability of cell to proliferate, thereby retaining its reproduction ability to form a large colony (> 50 cells) or a clone [51]. L-

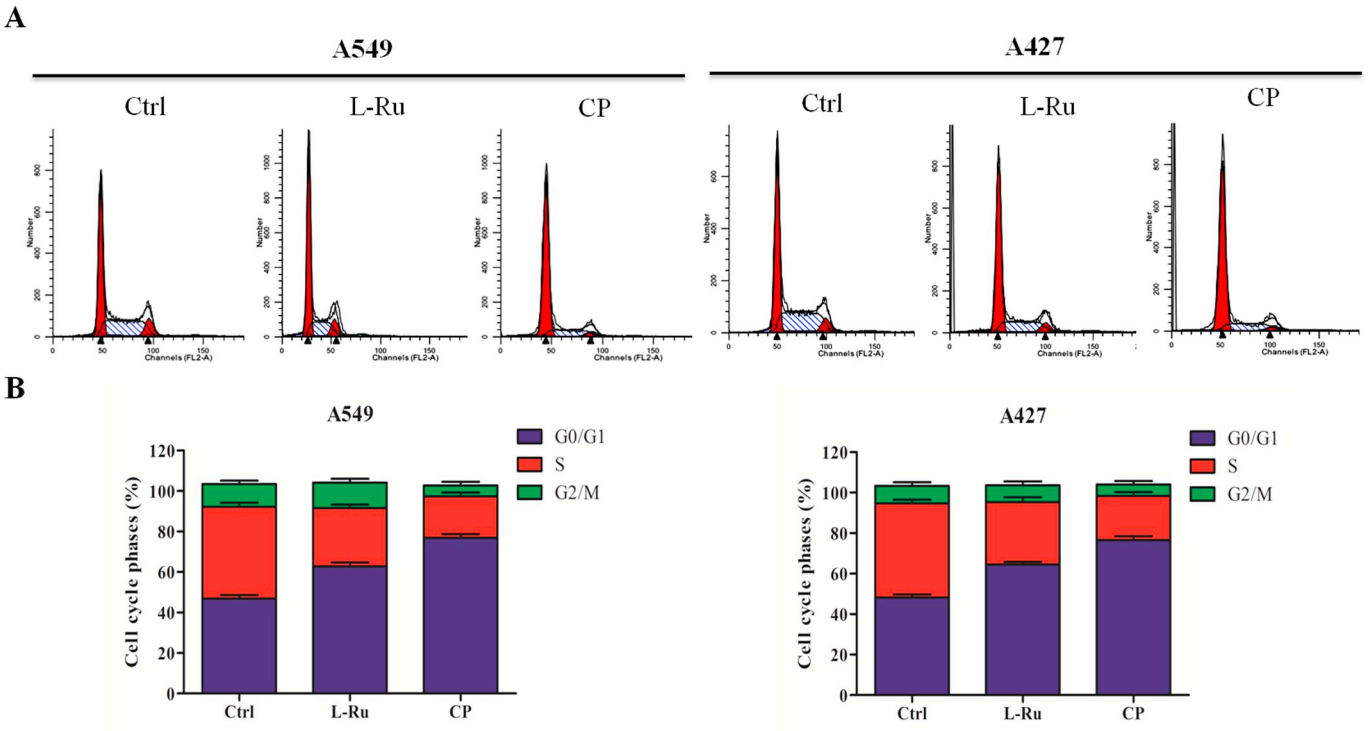

Fig. 4. L-Ru interfere with cell cycle in NSCLC cells. (A) A549 and A427 cells were treated with 20 μM of L-Ru for 24 h. Representative histograms of PI staining were showed. (B) The percentage distribution of cell cycle phases of A549 and A427 cells. Values represented mean ± SD of three independent experiments.

Ru significantly inhibited the number of A549 and A427 colonies when compare with control (Fig. 1B and C).The CP (20 μM) abolished more dramatic capacity of NSCLC cells to form colonies.

The cell death by apoptosis is one of the main type of death and involves a series of biochemical events leading to marker changes in cellular morphology, including externalization of phosphatidylserine in the cellular membrane, chromatin condensation, membrane bleeding, nuclear breakdown, and the appearance of membrane-associated apoptotic bodies, and internucleosomal DNA fragmentation [52]. Morphological investigation confirmed the cell shrinkage, membrane bleeding, nuclear condensation and DNA fragmentation in treated A549 and A427 cells with L-Ru and/or CP used as a control, due to the fact

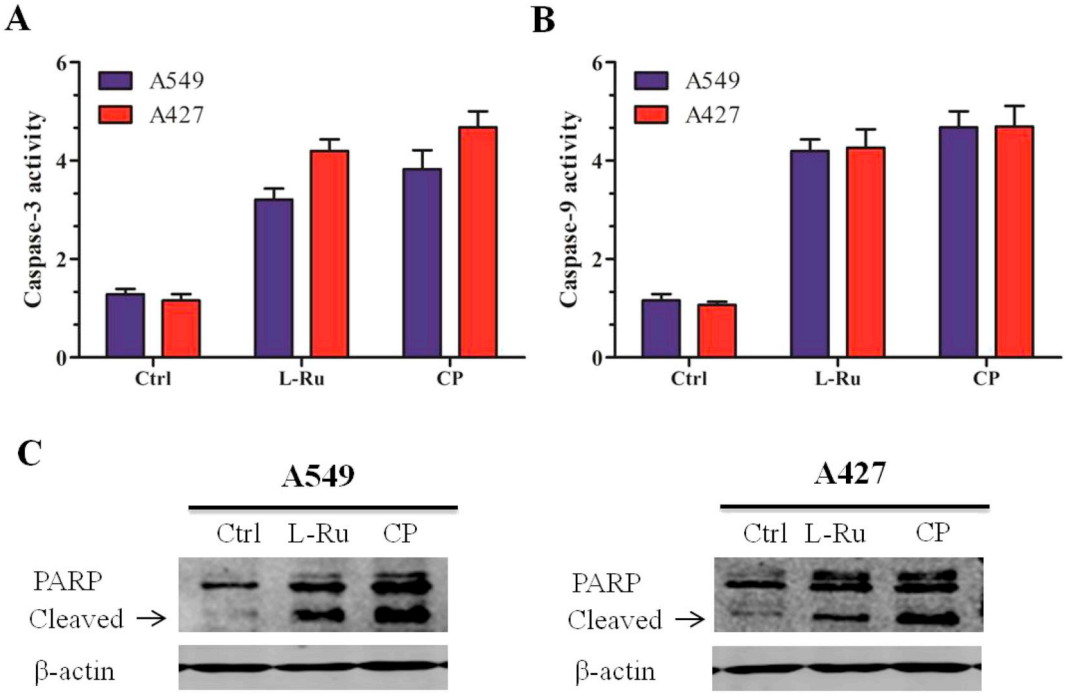

Fig. 5. Activation of caspase-3 and -9 signaling by ruthenium in NSCLC. A549 and A427 cells were treated with 20 μM of L-Ru or CP for 24 h. (A) caspase-3 and (B) caspase-9 activation was measured by colorimetric method. Values represented mean ± SD of three independent experiments. (C) A549 and A427 cells were treated with 20 μM of L-Ru or CP for 24 h and subjected to western blot against PARP antibody. β-actin was used as loading control.

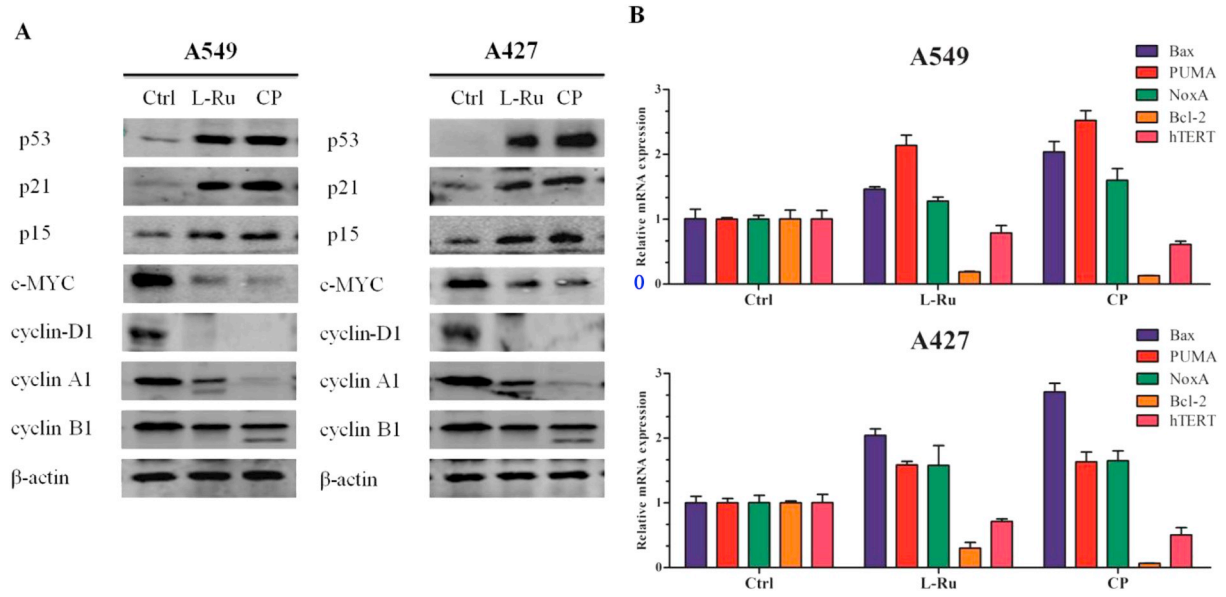

Fig. 6. Expression of apoptosis and cell cycle inhibition proteins by L-Ru. (A) A549 and A427 cells were treated with 20 μM of L-Ru for 24 h and subjected to western blot analysis against indicated antibodies. Appropriate controls were included: positive control (CP; 20 μM) and negative control DMSO (0.1%) were treated with cells for 24 h. β-actin was used as loading control. (B) A549 and A427 cells were treated with 20 μM of L-Ru for 24 h and mRNA expression of p53-traget genes were analyzed by qRT-PCR analysis. Error bars represent the average of three independent experiments (mean ± SD).

that it is well known for its potent apoptosis-inducing activities. As shown in Fig. 2, A549 and A427 cells indicated the apoptotic induction property of complex. Increased numbered of cell death by apoptosis seem to main mechanism behind anticancer property of L-Ru. To further, investigate the anticancer potential of L-Ru is associated with the induction of death by apoptosis or necrosis was determined, using Annexin V-FITC/PI staining. As shown in Fig. 3, treatment of cells with L-Ru (20 μM) exhibited 35.9% and 34.5% of A549 and A427 cells were in the apoptotic phase, respectively. The number of cells at the early and late apoptotic phases greatly increased, indicated that ruthenium complex potently induced apoptotic cell death.

Apoptotic induction and cell cycle regulation are intimately related to each other. The cell cycle arrest in the G0/G1 phase may have led to their apoptosis by disrupting the cell cycle. We demonstrated that A549 and A427 cells significantly arrest the cell in G0/G1 phase by inhibiting the cells entering into S-phase of the cell cycle (Fig. 4). Earlier studies of Ru-arene complexes have demonstrated the potential of these complexes to generate arrest in the sub-G1 phase of cell death *via* the apoptosis pathway against breast cancer cells [53]. The kinetics of cervical cancer (HeLa) cells treatment with $[Ru(tpy)(Nh)_3](CF_3SO_3)_2$ (tpy = 2,2′;6′,2″-terpyridine, Nh = Norharman) complex demonstrated relationship between percentage of cells in apoptosis and an increase of cell detected in sub-G1 phase [54]. Similarly, Gaiddon et al. [55] and Li et al. [56] showed that ruthenium complex induces G0/G1 phase arrest by the p53 activation. Furthermore, ruthenium (II)/polypyridine complex $[Ru(dmp)_2(AHPIP)(ClO_4)_2]$ (dmp = 2,9-dimethyl-1,10-phenanthroline, AHPIP = 2-(3-amino-4-hydroxylphenyl)imidazo[4,5-*f*][1,10] phenanthroline) against liver cancer (Bel-7402) cells, in which the complex induced cell cycle arrest followed by apoptosis [57,58].

Caspase-dependent signaling plays an important role in the induction of apoptosis, and activation of individual caspase, which finally triggers cell death pathway. We observed that *in vitro* activities of caspase-3/-9 were significantly increased with L-Ru treatment in A549 and A427 cells (Fig. 5A, B). PARP is a nuclear enzyme required for DNA repair, but during apoptosis transduction, PARP is deactivated by separation into small fragments which contributes to the suppression of its function [59,60]. The observed elevated levels of cleaved PARP and active p53, together with apoptotic nuclei, indicate the cytotoxicity of ruthenium on NSCLC. We also evaluated the expression of PARP cleaved protein after 24 h of incubation of L-Ru by Western Blot (Fig. 5C). The results indicated that L-Ru obviously activated caspase3/9 and induced remarkable cleaved of PARP in NSCLC cells. This strongly demonstrated that L-Ru can induce cell death adjusted through caspase-dependent pathway.

In this article, the changes in gene expression of p53 were essential to better understand the mechanism by which L-Ru may acts in NSCLC cells. In normal conditions, p53 is maintained at a quite low-level expression, with its protein interacting with the proteasome. Activation of p53 promotes cell cycle arrest to allow DNA repair and/or apoptosis [61]. p21 is a tumor suppressor that inhibits cell cycle progression by decreasing DNA synthesis. Induction of p21 in response to chemotherapeutic agents is important in inhibition of cancer cell invasion, migration and metastasis [62,63]. Our data indicated that L-Ru induced the protein expression of p53, p21, and p15 in NSCLC cells. On the other hand, c-MYC oncogene expression was inhibited *via* p53 (Fig. 6A). c-MYC is a multifunctional gene important in cell cycle progression, apoptosis and cellular transformation. c-MYC amplification play critical role in cancer metastasis [64,65].

Several genes are involved in this process of apoptosis, which is operated by anti-apoptotic and pro-apoptotic genes regulation in response to genotoxic stress such as Bax, PUMA, and NoxA [66]. PUMA acts as a tumor suppressor gene that inhibits apoptosis and inhibits cell cycle progression [67]. qRT-PCR analyses were performed in lung cancer cells treated with L-Ru. Strong expression of Bax, PUMA, and NoxA were showed the ability of L-Ru to induce these genes (Fig. 6B). In contrast, qRT-PCR analysis showed that L-Ru greatly repressed the expression of hTERT and pro-apoptosis Bcl-2 oncogenes in lung cancer cells (Fig. 6B).

Cell invasion and migration are considered most critical steps for progression of cancer metastasis. Inhibition of cell migration and invasion play key roles in the suppression of both primary and secondary metastasis. *In vitro* migration assays are necessary to understand the mechanism of cell migration and also to identify the inhibitory or stimulatory capacity of the compounds [68]. The effect of ruthenium complex and CP (positive control) on NSCLC (A549 and A427 cells) cell migration was evaluated using Boyden chamber transwell migration and invasion assay, and a significant inhibition of cell migration as well as invasion was observed in both cell lines (Fig. 7). Previous studies

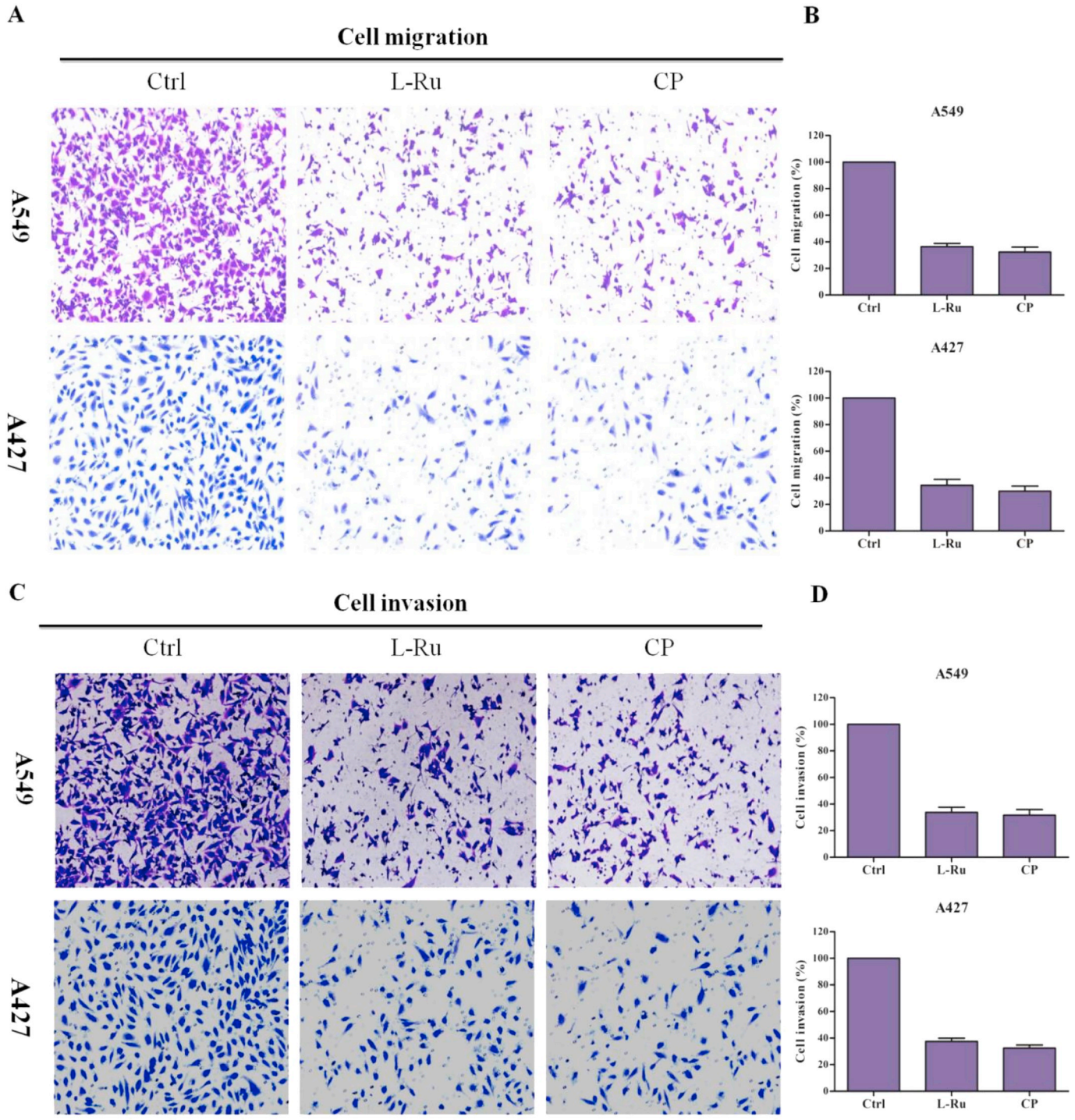

Fig. 7. Effects of L-Ru on migration and invasion of cancer cells. (A) A549 and A427 cells were treated with 20 μM of L-Ru or CP for 24 h and subjected to cell migration assay. (B) Represents statistical analysis of three independent experiments. (C) A549 and A427 cells were treated with 20 μM of L-Ru or 20 μM of CP for 24 h and subjected to cell invasion assay. (D) Represents statistical analysis of three independent experiments.

have shown that organometallic ruthenium complexes, such as Ru(II)-benzene-phenylimidazole [69], [Ru(η^6-*p*-cymene)Cl_2(PTA)] (RAPTA-C) (PTA = 1,3,5-triaza-7-phosphatricyclo-[3.3.1.1]decane), [Ru(η^6-*p*-cymene)Cl_2(DAPTA)] (DAPTA-C) (DPATA = 3,7-diacetyl-1,3,7-triaza-5-phosphabicyclo[3.3.1]nonane) [70], and Ru(II)-*p*-cymene-amino oxime [71], exhibited similar migration inhibitory capabilities in breast cancer cells and other tumor cell lines.

4. Conclusion

In summary, a dimetallic Ru-cymene complex appended on bis-pyrimidine (L-Ru) was synthesized and characterized by detailed spectroscopic and spectrophotometric analyses. The stability analysis showed it a stable complex in solution state in water/DMSO mixture. This study revealed that L-Ru possessed good cytotoxic activity and cell apoptosis against NSCLC. The underlying mechanism is believed to be through the upregulation of the tumor suppressor gene p53, which resulted in the imbalance of apoptosis regulatory protein causing

suppression of cancer cell growth, invasion and migration by blocking cell cycle progression and downregulation of oncogenes. PARP become activated and cleaved their substrates, thus initiating the cells apoptotic machinery. Overall, our results indicated that L-Ru was a very promising candidate for future studies aiming at understanding its mechanism of action in order to investigate it potential use as a new anticancer agent in NSCLC therapy.

5. Material and methods

5.1. Reagents and cell culture

All analytical grade reagents were purchased from commercial sources and used without further purification. Dichloro(*p*-cymene)ruthenium(II) dimer was purchased from Energy Chemical Shanghai China. Preparative thin layer chromatography (TLC) was performed on precoated silica gel plates (0.4–0.5 mm thick). ^{1}H, and ^{13}C NMR analyses were performed using Bruker AVANCE III HD 400 MHz spectrophotometer. Positive ions HR-ESIMS analyses were performed using Bruker micrOTOF II.

Reagents for cell culture system were purchased from GIBCO BRL (Grand Island, NY, USA). Cisplatin (*cis*-diamminedichloroplatinum II), Hoechst-33342, 3-(4,5-Dimethylthiazol-2-yl)-2,5-diphenyltetra-zolium bromide (MTT) were purchased from Sigma-Aldrich, St. Louis, USA. The terminal deoxynucleotidyl transferase dUTP nick end labeling (TUNEL) assay kit was purchased from Roche Applied Science. Antibodies for poly (ADP-ribose) polymerase (PARP), p53, p21, p15, c-MYC, cyclin D1, cyclin A1, cyclin B1, and beta-actin were obtained from Cell Signaling technology (Beverly, MA, USA).

NSCLC A549 and A427 cells were obtained from American Type Culture Collection (ATCC, Manassas, VA, USA). Cells were cultured in RPMI-1640 medium supplemented with 10% fatal bovine serum (FBS), 100 U/mL penicillin and 100 μg/mL streptomycin. The cells were maintained at 37 °C under a humidified atmosphere of 5% CO_2.

5.2. Synthesis of bis-pyrimidine based ligand (L)

92 mg 4 equivalents of Na was dissolved in 20 mL dry n-propanol in a 100 mL round bottom flask at RT. 208 mg 2.2 equivalents of acetamidine hydrochloride was added to the Na solution in one portion followed by 341 mg, 1 equivalent of the bis-chalcone (Chal). The temperature of the mixture was slowly raised to reflux and stirred for 18 h. The mixture was cooled to RT, added with 20 mL of water and stirred at RT for 1 h, which resulted in a white solid precipitation. The solid was filtered, washed with water and recrystallized from EtOH/water 3:1 mixture. 230 mg pure L was recovered in 55% yield. L was characterized as below while the IR, ^{1}H, ^{13}C NMR and ESI-MS spectra were given in the ESI. FT-IR (KBr Pellet) cm^{-1}: 3506, 1595, 1575, 1537, 1473, 1450, 1435, 1397, 1381, 1363, 1271, 1086, 992, 829, 801, 763, 743, 673, 650, 638, 623. ^{1}H NMR (400 MHz, $CDCl_3$) δ 9.37 (s, 2H), 8.83 (d, J = 4.8 Hz, 2H), 8.65 (d, J = 7.7 Hz, 2H), 8.54 (d, J = 7.8 Hz, 2H), 8.05 (t, J = 7.9 Hz, 1H), 7.90 (t, J = 7.6 Hz, 2H), 7.46–7.41 (m, 2H), 2.93 (s, 6H) ppm. ^{13}C NMR (100 MHz, $CDCl_3$) δ 167.9, 164.2, 163.9, 154.7, 154.4, 149.6, 138.0, 137.0, 125.0, 123.1, 121.9, 111.3, 26.3 ppm. HR-MS (ESI): Calcd. chemical formula: $C_{25}H_{20}N_7$, $[M + H]^+$, 418.1780, found 418.1775.

5.3. Synthesis of Ru(II) complex (L-Ru)

A two necked round bottom flask with a magnetic stirrer bar was charged with 66 mg 2.2 equivalents of ruthenium(cymene)dichloride dimer and 20 mL of CH_3OH/CH_2Cl_2 (1:1) mixture. The flask was immersed in an oil bath preheated at 40 °C. 41.7 mg of L dissolved in 10 mL CH_3OH/CH_2Cl_2 (1:1) mixture was added drop wise to the flask and stirring was continued at the same temperature for 24 h. The mixture was cooled to RT and vacuum evaporated to get a red sticky solid. The solid was dissolved in 20 mL ethanol, excess (200 mg) NH_4PF_6 dissolved in 20 mL water was added to it that resulted in a greenish yellow solid precipitate. The solid was filtered and washed with a 1:1 mixture of ethanol/water and dried in vacuum. 103 mg solid complex (L-Ru) was recovered in 82% yield. FT-IR (KBr Pellet) cm^{-1}: 3451, 1597, 1532, 1485, 1439, 1402, 1385, 842, 792, 753, 641, 558. ^{1}H NMR (400 MHz, Acetonitrile-d_3) δ 9.38 (d, J = 5.3 Hz, 2H), 9.34 (d, J = 5.7 Hz, 2H), 8.87–8.84 (m, 4H), 8.36 (t, J = 7.9 Hz, 3H), 7.89 (t, J = 6.5 Hz, 2H), 6.10 (d, J = 3.6 Hz, 2H), 5.92 (d, J = 6.2 Hz, 2H), 5.84 (d, J = 6.1 Hz, 2H), 5.76 (d, J = 6.1 Hz, 2H), 3.43 (d, J = 2.0 Hz, 6H), 2.60–2.45 (m, 2H), 2.30 (s, 6H), 0.99 (d, J = 6.9 Hz, 6H), 0.94 (d, J = 6.9 Hz, 6H) ppm. ^{13}C NMR (100 MHz, DMSO-d_6) δ 172.3, 163.6, 158.5, 156.9, 153.5, 152.2, 140.7, 130.1, 127.4, 126.0, 112.9, 106.8, 105.2, 89.0, 85.6, 85.3, 82.6, 30.8, 30.3, 22.4, 22.0, 19.0 ppm. Anal. found (calculated for $C_{45}H_{47}Cl_2N_7Ru_2.2PF_6$): C, 43.32 (43.28); 3.82H, (3.79); N, 7.81 (7.85). HR-MS (ESI): Calcd. for chemical formula: $[C_{45}H_{47}Cl_2N_7Ru_2]^{2+}$, $[M\text{-}2PF_6]^{2+}$ 479.5673, found 479.5691.

5.4. MTT assay

The 3-(4,5-dimethylthiazol-2-yl)-2,5-diphenyltetrazolium bromide (MTT) assay (Sigma-Aldrich, St. Louis, MO, USA) was used to determine the cell proliferation and viability, the cells were seeded at a density of 5×10^3 cells/well and were allowed to adhere prior to exposure to test substrate for 24 h. Then, 20 μL of 1 mg/mL MTT (Sigma-Aldrich) was added, and the cells were incubated in a humidified atmosphere containing 5% CO_2 at 37 °C for 4 h. The supernatant was then removed and formazan crystals were dissolved in 200 μL of di-methyl sulfoxide (DMSO; Sigma-Aldrich) for 15 min. Optical density was determined at a wavelength of 570 nm using a micro-plate reader (Biotek, Winooski, VT, USA). The viability of the non-treated cells (control) was defined as 100%, and the viability of cells from all other groups was calculated separately from that of the control group.

5.5. Colony formation assay

A549 and A427 cells were seeded at a counteraction of 500 cells/mL into 6-well plates. After 24 h of seeding, cells were treated with 20 μM of L-Ru and incubated for 24 h, when cells were washer with PBS and medium was replaced with fresh medium. The positive control cells were treated with cisplatin and negative control was treated with 0.1% of DMSO. After, 14 days, cells were washed with PBS and fixed with glutaraldehyde 6% (*v*/v) and crystal violet 0.5% (w/v) for 3 h. Then cells were washed with PBS and plate images were taken under light microscope.

5.6. Chromatin staining by Hoechst-33342

To determine the DNA chromatin morphological features, A549 and A427 cells were exposed to Hoechst-3332 stain according to Rahman et al. [37]. Briefly, the cells were cultured and treated with either cisplatin and/or L-Ru (20 μM) for 24 h, washed with PBS (pH 8.0), and fixed with cold 4% paraformaldehyde (PFA). Cells were washed with PBS again and incubated with Hoechst-33342 (1 μg/mL) at room temperature for 15 min. After washing with PBS, the resulting fluorescence was detected under the fluorescence microscope (Olympus, Tokyo, Japan) at 20× magnification.

5.7. Determination of acridine orange/ethidium bromide (AO/EB) staining

After treatment with 20 μM of cisplatin and/or L-Ru for 24 h, cells were washed with PBS and stain with 100 mg/mL of acridine orange and incubated at room temperature for 15 min. After washing with PBS fluorescent micrographs were obtained at 20× magnification using fluorescence microscope (Nikon, Tokyo Japan).

5.8. Cell apoptosis analysis by flow cytometry

The cell apoptosis was analyzed by flow cytometry using Annexin V-fluorescein isothiocyanate (FITC) an apoptosis detection kit (BD Pharmingen), according to the manufacturer's instructions. In brief, after the indicated treatments, cells were collected and centrifuged. The cell pellets were resuspended in 1 × binding buffer at a concentration of 1×10^6 cells/mL. Cell suspension (100 μL) was incubated with 5 μL Annexin V-FITC for 15 min in the dark. Subsequently, propidium iodide (PI; 10 μL) was added to cell suspension in dark for 30 min. Apoptosis was analyzed by FASC using the Cell-Quest software (Beckman Coulter).

5.9. Terminal transferase-mediated dUTP nick end labeling (TUNEL) assay

Cell apoptosis of the tumor cells was detected by TUNEL assay using an *In Situ* Cell Death Detection Kit (Roche Diagnostic, Mannheim, Germany) according to the manufacturer's instructions. In brief, the cells were incubated with the TUNEL reaction mixture at 37 °C for 1 h in dark. Labeled DNA was visualized with an anti-fluorescein antibody conjugated with peroxidase using 3,3′-diaminobenzidine (Sigma). For negative control, TdT was omitted from the reaction mixture. TUNEL-positive cells were imaged and mounted by a light microscope and expressed as a percentage of the total cells.

5.10. Flow cytometry analysis of cell cycle

Cells were collected at a density of 90% after culture, fixed in 70% cold ethanol and kept at 4 °C for 3 h. The cells were washed with PBS and resuspended in staining buffer containing 25 μL of propidium iodide and 10 μL of RNase A. the cell suspension was incubated for 45 min in dark at 37 °C, before analysis of cell cycle markers by fluorescence activated cell sorting (FACS) caliber flow cytometry (BD, Franklin Lakes, NJ, USA).

5.11. Western blot analysis

Proteins were extracted from the cultured cells with indicated treatments, cells were washed with 1× phosphate-buffered saline (PBS), and lysated in NP-40 buffer supplemented with protease inhibitor cocktail and phosphate inhibitor cocktail (Sigma-Aldrich), and centrifuged at 12000 RPM for 10 min at 4 °C. Protein concentration was determined by the bicinchoninic acid (BCA) protein assay Kit (Pierce, Rockford, IL, USA). Equal amounts of proteins were separated by sodium dodecyl sulfate-polyacrylamide gel electrophoresis (SDS-PAGE) and transferred to nitrocellulose membrane (Bio-Rad laboratories, Inc., Hercules, CA, USA). The membranes were blocked for non-specific binding with 5% non-fat dry milk in phosphate-buffered saline contain 0.05% Tween-20 (PBST) for 1 h at room temperature, the blots were incubated with primary antibodies (against PARP, p53, p21, p15, cyclin D1, cyclin B1, cyclin A1, c-MYC, and β-actin) at 4 °C overnight. Blots were washed with PBST three times and incubated with secondary antibodies (anti-mouse or anti-rabbit; 1:5000 dilution) for 1 h. Then blots were washed again three times and exposed to Odyssey LI-COR-scanner (LI-COR Biotechnology, Lincoln, NE, USA).

5.12. RNA extraction and SYBR green quantitative PCR analysis

Total RNA was extracted from cells using Trizol reagent (Invitrogen, CA, USA) according to the manufacturer's instructions. cDNA was synthesized from equal amount of RNA using the PrimeScript™ RT reagent kit (TaKaRa, Otsu, Shiga, Japan) according to the manufacturer's protocol. Quantitative PCR was performed using SYBR Premix Ex Taq II (TaKaRa) on an ABI 7500 Real-Time PCR system (Applied Biosystems). The relative gene expression was calculated using the $2^{-\Delta\Delta CT}$ method. The β-actin was used as the internal control. RT-PCR primer sequence is given in the Table S1.

5.13. Caspase activity assay

Caspase-3 and caspase-9 activities were determined by spectrophotometric method (Caspase Assay Kit, Beyotime, Jiangsu, China). Treated cells were, suspended in cell lysis buffer (100 μL) and incubated on ice for 30 min, after centrifugation at 10,000 ×g for 15 min at 4 °C, supernatants were collected and placed in 96-well plats and then 10 μL of specific caspase substrates (Ac-DEVD-*p*NA) was added. Plated were incubated at 37 °C for 2 h and caspase activities were tested by spectrophotometer.

5.14. Cell migration and invasion assays

Cells migration and invasion were determined by Transwell Boyden chamber (8-μm pore size; Corning Costar, NY, USA) method. For migration assay, the cells (2×10^5) were treated with L-Ru or cisplatin for 24 h, then digest and seeded in to transwell chamber for 24 h. The invasion assay, the members of the upper chamber were precoated with Martigel (Sigma-Aldrich, St. Louis, USA), then cells were added into upper chamber containing with free-serum RPMI-1640. In the both assays, 700 μL of RPMI-1640 with 10% FBS (serum media) was added to the lower chamber of chemotaxis. After incubation for 24 h, cells on the upper membrane were removed and those migrated or invaded through the membranes were fixed with 4% PFA and stained with crystal violet (Sigma-Aldrich). Five randomly selected fields were observed under a fluorescence microscope (Olympus), and the average was calculated.

Abbreviations

MTT	3-(4,5-dimethylthiazol-2-yl)-2,5-diphenyltetrazolium bromide
PARP	Poly (ADP-ribose) polymerase
Caspase	Cysteine-dependent aspartate-directed protease
TUNEL	Terminal deoxynucleotidyl transferase dUTP nick end labeling
V-FITC	Annexin V-fluorescein isothiocyanate conjugate
c-MYC	Myelocytomatosis
qRT-PCR	Quantitative real-time polymerase chain reaction
BAX	B-cell lymphoma 2 associated X, Apoptosis Regulator
Bcl2	B-cell lymphoma 2
hTERT	Telomerase reverse transcriptase
NoxA	Phorbol-12-myristate-13-acetate-induced protein 1
PUMA	p53 upregulated modulator of apoptosis
AHPIPO	2-(3-amino-4-hydroxylphenyl)imidazo[4,5-*f*][1,10]phenanthroline
dmp	2,9-dimethyl-1,10-phenanthroline
BzCN	benzonitrile
bipy	2,2′-bipyridine
dppe	1,2-bis(diphenylphosphino) ethane
typ	2,2′;6′,2″-terpyridine
Nh	Norharman
RAPTA	[Ru(η^6-arene)X2(PTA)] (PTA = 1,3,5-triaza7-phosphaadamantane)
RAPTA-C	[Ru(η^6-*p*-cymene)Cl_2(PTA)]
DAPTA	3,7-diacetyl-1,3,7-triaza-5-phosphabicyclo[3.3.1]nonane
DAPTA-C	[Ru(η^6-*p*-cymene)Cl_2(DAPTA)]
AHPIP	2-(3-amino-4-hydroxylphenyl)imidazo[4,5-*f*][1,10]phenanthroline
N-N	Dinitrogen donor ligands

Acknowledgements

This work was supported by National Natural Science Foundation of China (Grant No. 31672247).

Appendix A. Supplementary data

^{1}H and ^{13}C NMR spectra, MS chromatograms and IR spectra for all compounds, stability ^{1}H NMR comparative spectra plot, RT-PCR primer sequence table and other supplementary data associated with this article can be found in the online version at https://doi.org/10.1016/j.jinorgbio.2019.01.019.

References

[1] I. Potocnjak, I. Gobin, R. Domitrovic, Carvacrol induces cytotoxicity in human cervical cancer cells but causes cisplatin resistance: involvement of MEK-ERK activation, Phytother. Res. (2018) 1–8.

[2] L.F. Magalhaes, F. Mello-Andrade, W.C. Pires, H.D. Silva, P.F.F. da Silva, L.M. Macedo, C. Henrique de Castro, C.C. Carneiro, C.G. Cardoso, P.R. de Melo Reis, L. Camargo de Oliveira, R.R. Caetano, A.A. Batista, E.P. Silveira-Lacerda, cis-[RuCl(BzCN)(bipy)(dppe)]PF6 induces anti-angiogenesis and apoptosis by a mechanism of caspase-dependent involving DNA damage, PARP activation, and Tp53 induction in Ehrlich tumor cells, Chem. Biol. Interact. 278 (2017) 101–113.

[3] R.L. Siegel, K.D. Miller, A. Jemal, Cancer statistics, 2017, CA Cancer J. Clin. 67 (1) (2017) 7–30.

[4] O. Wattanathamsan, S. Treesuwan, B. Sritularuk, V. Pongrakhananon, Cypripedin, a phenanthrenequinone from Dendrobium densiflorum, sensitizes non-small cell lung cancer H460 cells to cisplatin-mediated apoptosis, J. Nat. Med. (2018) 1–11.

[5] K.D. Miller, R.L. Siegel, C.C. Lin, A.B. Mariotto, J.L. Kramer, J.H. Rowland, K.D. Stein, R. Alteri, A. Jemal, Cancer treatment and survivorship statistics, 2016, CA Cancer J. Clin. 66 (4) (2016) 271–289.

[6] D.S. Ettinger, W. Akerley, H. Borghaei, A.C. Chang, R.T. Cheney, L.R. Chirieac, T.A. D'Amico, T.L. Demmy, R. Govindan, F.W. Grannis, S.C. Grant, L. Horn, T.M. Jahan, R. Komaki, F.-M. Kong, M.G. Kris, L.M. Krug, R.P. Lackner, I.T. Lennes, B.W. Loo, R. Martins, G.A. Otterson, J.D. Patel, M.C. Pinder-Schenck, K.M. Pisters, K. Reckamp, G.J. Riely, E. Rohren, T.A. Shapiro, S.J. Swanson, K. Tauer, D.E. Wood, S.C. Yang, K. Gregory, M. Hughes, Non–small cell lung cancer, version 2, 2013, Journal of the National Comprehensive Cancer Network 11 (6) (2013) 645–653.

[7] C.C. Chen, C.P. Kao, M.M. Chiu, S.H. Wang, The anti-cancer effects and mechanisms of Scutellaria barbata D. Don on CL1-5 lung cancer cells, Oncotarget 8 (65) (2017) 109340–109357.

[8] S.A. Patil, S.A. Patil, R. Patil, R.S. Keri, S. Budagumpi, G.R. Balakrishna, M. Tacke, N-heterocyclic carbene metal complexes as bio-organometallic antimicrobial and anticancer drugs, Future Med. Chem. 7 (10) (2015) 1305–1333.

[9] A. Markowska, B. Kasprzak, K. Jaszczynska-Nowinka, J. Lubin, J. Markowska, Noble metals in oncology, Contemp. Oncol. (Pozn.) 19 (4) (2015) 271–275.

[10] R.P. Miller, R.K. Tadagavadi, G. Ramesh, W.B. Reeves, Mechanisms of cisplatin nephrotoxicity, Toxins (Basel) 2 (11) (2010) 2490–2518.

[11] L. Kelland, The resurgence of platinum-based cancer chemotherapy, Nat. Rev. Cancer 7 (8) (2007) 573–584.

[12] A.M. Florea, D. Busselberg, Cisplatin as an anti-tumor drug: cellular mechanisms of activity, drug resistance and induced side effects, Cancers (Basel) 3 (1) (2011) 1351–1371.

[13] D. Kovala-Demertzi, A. Papageorgiou, L. Papathanasis, A. Alexandratos, P. Dalezis, J.R. Miller, M.A. Demertzis, In vitro and in vivo antitumor activity of platinum(II) complexes with thiosemicarbazones derived from 2-formyl and 2-acetyl pyridine and containing ring incorporated at N(4)-position: synthesis, spectroscopic study and crystal structure of platinum(II) complexes with thiosemicarbazones, potential anticancer agents, Eur. J. Med. Chem. 44 (3) (2009) 1296–1302.

[14] K. Cheung-Ong, G. Giaever, C. Nislow, DNA-damaging agents in cancer chemotherapy: serendipity and chemical biology, Chem. Biol. 20 (5) (2013) 648–659.

[15] M.P. Singh, A.K. Chauhan, S.C. Kang, Morin hydrate ameliorates cisplatin-induced ER stress, inflammation and autophagy in HEK-293 cells and mice kidney via PARP-1 regulation, Int. Immunopharmacol. 56 (2018) 156–167.

[16] F.U. Rahman, A. Ali, R. Guo, W.K. Wang, H. Wang, Z.T. Li, Y. Lin, D.W. Zhang, Efficient one-pot synthesis of trans-Pt(II)(salicylaldimine)(4-picoline)Cl complexes: effective agents for enhanced expression of p53 tumor suppressor genes, Dalton Trans. 44 (21) (2015) 9872–9880.

[17] X. Yang, L. Chen, Y. Liu, Y. Yang, T. Chen, W. Zheng, J. Liu, Q.Y. He, Ruthenium methylimidazole complexes induced apoptosis in lung cancer A549 cells through intrinsic mitochondrial pathway, Biochimie 94 (2) (2012) 345–353.

[18] X. Meng, M.L. Leyva, M. Jenny, I. Gross, S. Benosman, B. Fricker, S. Harlepp, P. Hebraud, A. Boos, P. Wlosik, P. Bischoff, C. Sirlin, M. Pfeffer, J.P. Loeffler, C. Gaiddon, A ruthenium-containing organometallic compound reduces tumor growth through induction of the endoplasmic reticulum stress gene CHOP, Cancer Res. 69 (13) (2009) 5458–5466.

[19] B. Saygideger Demir, T. Keles, O. Serindag, Antioxidant enzyme inhibitor role of phosphine metal complexes in lung and leukemia cell lines, Bioinorg. Chem. Appl. 2014 (717421) (2014) 1–10.

[20] F. Li, J.G. Collins, F.R. Keene, Ruthenium complexes as antimicrobial agents, Chem. Soc. Rev. 44 (8) (2015) 2529–2542.

[21] C. Mari, V. Pierroz, R. Rubbiani, M. Patra, J. Hess, B. Spingler, L. Oehninger, J. Schur, I. Ott, L. Salassa, S. Ferrari, G. Gasser, DNA intercalating Ru(II) polypyridyl complexes as effective photosensitizers in photodynamic therapy, Chemistry 20 (44) (2014) 14421–14436.

[22] Q.X. Zhou, Y. Zheng, T.J. Wang, Y.J. Chen, K. Li, Y.Y. Zhang, C. Li, Y.J. Hou, X.S. Wang, A novel azopyridine-based Ru(II) complex with GSH-responsive DNA photobinding ability, Chem. Commun. (Camb.) 51 (53) (2015) 10684–10686.

[23] M.A. Sgambellone, A. David, R.N. Garner, K.R. Dunbar, C. Turro, Cellular toxicity induced by the photorelease of a caged bioactive molecule: design of a potential dual-action Ru(II) complex, J. Am. Chem. Soc. 135 (30) (2013) 11274–11282.

[24] J.J. Soldevila-Barreda, I. Romero-Canelon, A. Habtemariam, P.J. Sadler, Transfer hydrogenation catalysis in cells as a new approach to anticancer drug design, Nat. Commun. 6 (1) (2015) 6582–6589.

[25] Z.F. Chen, Q.P. Qin, J.L. Qin, J. Zhou, Y.L. Li, N. Li, Y.C. Liu, H. Liang, Water-soluble ruthenium(II) complexes with chiral 4-(2,3-dihydroxypropyl)-formamide oxoaporphine (FOA): in vitro and in vivo anticancer activity by stabilization of G-quadruplex DNA, inhibition of telomerase activity, and induction of tumor cell apoptosis, J. Med. Chem. 58 (11) (2015) 4771–4789.

[26] H. Huang, P. Zhang, B. Yu, Y. Chen, J. Wang, L. Ji, H. Chao, Targeting nucleus DNA with a cyclometalated dipyridophenazineruthenium(II) complex, J. Med. Chem. 57 (21) (2014) 8971–8983.

[27] A. Grozav, O. Balacescu, L. Balacescu, T. Cheminel, I. Berindan-Neagoe, B. Therrien, Synthesis, anticancer activity, and genome profiling of thiazolo arene ruthenium complexes, J. Med. Chem. 58 (21) (2015) 8475–8490.

[28] V. Pierroz, T. Joshi, A. Leonidova, C. Mari, J. Schur, I. Ott, L. Spiccia, S. Ferrari, G. Gasser, Molecular and cellular characterization of the biological effects of ruthenium(II) complexes incorporating 2-pyridyl-2-pyrimidine-4-carboxylic acid, J. Am. Chem. Soc. 134 (50) (2012) 20376–20387.

[29] A. Frei, R. Rubbiani, S. Tubafard, O. Blacque, P. Anstaett, A. Felgentrager, T. Maisch, L. Spiccia, G. Gasser, Synthesis, characterization, and biological evaluation of new Ru(II) polypyridyl photosensitizers for photodynamic therapy, J. Med. Chem. 57 (17) (2014) 7280–7292.

[30] C.S. Menezes, L.C. de Paula Costa, V. de Melo Rodrigues Avila, M.J. Ferreira, C.U. Vieira, L.A. Pavanin, M.I. Homsi-Brandeburgo, A. Hamaguchi, E. de Paula Silveira-Lacerda, Analysis in vivo of antitumor activity, cytotoxicity and interaction between plasmid DNA and the cis-dichloro-tetra-amine-ruthenium(III) chloride, Chem. Biol. Interact. 167 (2) (2007) 116–124.

[31] A.P. de Lima, C. Pereira Fde, C.A. Vilanova-Costa, F.M. Mello, S. Ribeiro Ade, P.L. Benfica, M.C. Valadares, L.A. Pavanin, W.B. dos Santos, P. Lacerda Ede, The compound cis-(dichloro)tetramineruthenium(III) chloride induces caspase-mediated apoptosis in K562 cells, Toxicol. in Vitro 24 (6) (2010) 1562–1568.

[32] C.A. Vilanova-Costa, H.K. Porto, C. Pereira Fde, A.P. de Lima, W.B. Dos Santos, P. Silveira-Lacerda Ede, The ruthenium complexes cis-(dichloro)tetramineruthenium(III) chloride and cis-tetraammine(oxalato)ruthenium(III) dithionate overcome resistance inducing apoptosis on human lung carcinoma cells (A549), Biometals 27 (3) (2014) 459–469.

[33] H.K.P. Porto, C.A.S.T. Vilanova-Costa, F.M. dos Santos Mello, W.L. da Costa, A.P. de Lima, F. de Castro Pereira, M.A.P. Almeida, A.E. Graminha, A.A. Batista, E. de Paula Silveira-Lacerda, Synthesis of a ruthenium(II) tryptophan-associated complex and biological evaluation against Ehrlich murine breast carcinoma, Transit. Met. Chem. 40 (1) (2014) 1–10.

[34] R.M. Lord, A.J. Hebden, C.M. Pask, I.R. Henderson, S.J. Allison, S.L. Shepherd, R.M. Phillips, P.C. McGowan, Hypoxia-sensitive metal beta-ketoiminato complexes showing induced single-strand DNA breaks and cancer cell death by apoptosis, J. Med. Chem. 58 (12) (2015) 4940–4953.

[35] Y. Huang, W. Huang, L. Chan, B. Zhou, T. Chen, A multifunctional DNA origami as carrier of metal complexes to achieve enhanced tumoral delivery and nullified systemic toxicity, Biomaterials 103 (2016) 183–196.

[36] T. Chen, W.-J. Mei, Y.-S. Wong, J. Liu, Y. Liu, H.-S. Xie, W.-J. Zheng, Chiral ruthenium polypyridyl complexes as mitochondria-targeted apoptosis inducers, MedChemComm 1 (1) (2010) 73–75.

[37] F.U. Rahman, M.Z. Bhatti, A. Ali, H.Q. Duong, Y. Zhang, B. Yang, S. Koppireddi, Y. Lin, H. Wang, Z.T. Li, D.W. Zhang, Homo- and heteroleptic Pt(II) complexes of ONN donor hydrazone and 4-picoline: a synthetic, structural and detailed mechanistic anticancer investigation, Eur. J. Med. Chem. 143 (2018) 1039–1052.

[38] F.U. Rahman, A. Ali, I.U. Khan, H.Q. Duong, S.B. Yu, Y.J. Lin, H. Wang, Z.T. Li, D.W. Zhang, Morpholine or methylpiperazine and salicylaldimine based heteroleptic square planner platinum (II) complexes: in vitro anticancer study and growth retardation effect on E. coli, Eur. J. Med. Chem. 131 (2017) 263–274.

[39] F.U. Rahman, A. Ali, I.U. Khan, H.Q. Duong, R. Guo, H. Wang, Z.T. Li, D.W. Zhang, Novel phenylenediamine bridged mixed ligands dimetallic square planner Pt(II) complex inhibits MMPs expression via p53 and caspase-dependent signaling and suppress cancer metastasis and invasion, Eur. J. Med. Chem. 125 (2017) 1064–1075.

[40] F.U. Rahman, A. Ali, R. Guo, Y.C. Zhang, H. Wang, Z.T. Li, D.W. Zhang, Synthesis and anticancer activities of a novel class of mono- and di-metallic Pt(II)(salicylaldiminato)(DMSO or Picolino)Cl complexes, Dalton Trans. 44 (5) (2015) 2166–2175.

[41] F.-U. Rahman, M.Z. Bhatti, A. Ali, H.-Q. Duong, Y. Zhang, X. Ji, Y. Lin, H. Wang, Z.-T. Li, D.-W. Zhang, Dimetallic Ru(II) arene complexes appended on bis-salicylaldimine induce cancer cell death and suppress invasion via p53-dependent signaling, Eur. J. Med. Chem. 157 (2018) 1480–1490.

[42] G. Suss-Fink, Arene ruthenium complexes as anticancer agents, Dalton Trans. 39 (7) (2010) 1673–1688.

[43] M.M. Haghdoost, J. Guard, G. Golbaghi, A. Castonguay, Anticancer activity and catalytic potential of ruthenium(II)-arene complexes with N,O-donor ligands, Inorg. Chem. 57 (13) (2018) 7558–7567.

[44] I. Cassells, T. Stringer, A.T. Hutton, S. Prince, G.S. Smith, Impact of various lipophilic substituents on ruthenium(II), rhodium(III) and iridium(III) salicylaldimine-based complexes: synthesis, in vitro cytotoxicity studies and DNA interactions, J. Biol. Inorg. Chem. 23 (5) (2018) 763–774.

[45] M.D. Hall, K.A. Telma, K.E. Chang, T.D. Lee, J.P. Madigan, J.R. Lloyd, I.S. Goldlust,

J.D. Hoeschele, M.M. Gottesman, Say no to DMSO: dimethylsulfoxide inactivates cisplatin, carboplatin, and other platinum complexes, Cancer Res. 74 (14) (2014) 3913–3922.
[46] W.H. Ang, E. Daldini, C. Scolaro, R. Scopelliti, L. Juillerat-Jeannerat, P.J. Dyson, Development of organometallic ruthenium-arene anticancer drugs that resist hydrolysis, Inorg. Chem. 45 (22) (2006) 9006–9013.
[47] K. Suntharalingam, S.G. Awuah, P.M. Bruno, T.C. Johnstone, F. Wang, W. Lin, Y.R. Zheng, J.E. Page, M.T. Hemann, S.J. Lippard, Necroptosis-inducing rhenium(V) oxo complexes, J. Am. Chem. Soc. 137 (8) (2015) 2967–2974.
[48] H.J. Kim, N. Hawke, A.S. Baldwin, NF-kappaB and IKK as therapeutic targets in cancer, Cell Death Differ. 13 (5) (2006) 738–747.
[49] A. Gornowicz, Z. Kaluza, A. Bielawska, H. Gabryel-Porowska, R. Czarnomysy, K. Bielawski, Cytotoxic efficacy of a novel dinuclear platinum(II) complex used with anti-MUC1 in human breast cancer cells, Mol. Cell. Biochem. 392 (1–2) (2014) 161–174.
[50] C. Pereira Fde, B.A. Lima, A.P. de Lima, W.C. Pires, T. Monteiro, L.F. Magalhaes, W. Costa, A.E. Graminha, A.A. Batista, J. Ellena, P. Siveira-Lacerda Ede, Cis-[RuCl(BzCN)(N-N)(P-P)]PF6 complexes: synthesis and in vitro antitumor activity, (BzCN = benzonitrile; N-N = 2,2′-bipyridine; 1,10-phenanthroline; P-P = 1,4-bis(diphenylphosphino) butane, 1,2-bis(diphenylphosphino)ethane, or 1,1′-(diphenylphosphino)ferrocene), J Inorg Biochem 149 (2015) 91–101.
[51] A. Munshi, M. Hobbs, R.E. Meyn, Clonogenic cell survival assay, in: R.D. Blumenthal (Ed.), Chemosensitivity: Volume 1 In Vitro Assays, Humana Press, Totowa, NJ, 2005, pp. 21–28.
[52] L. Galluzzi, I. Vitale, J.M. Abrams, E.S. Alnemri, E.H. Baehrecke, M.V. Blagosklonny, T.M. Dawson, V.L. Dawson, W.S. El-Deiry, S. Fulda, E. Gottlieb, D.R. Green, M.O. Hengartner, O. Kepp, R.A. Knight, S. Kumar, S.A. Lipton, X. Lu, F. Madeo, W. Malorni, P. Mehlen, G. Nunez, M.E. Peter, M. Piacentini, D.C. Rubinsztein, Y. Shi, H.U. Simon, P. Vandenabeele, E. White, J. Yuan, B. Zhivotovsky, G. Melino, G. Kroemer, Molecular definitions of cell death subroutines: recommendations of the Nomenclature Committee on Cell Death 2012, Cell Death Differ. 19 (1) (2012) 107–120.
[53] C.d.W. Hao, Mechanism and Disease, Springer New York Heidelberg Dordrecht, London, UK, 2014.
[54] Y. Chen, M.Y. Qin, J.H. Wu, L. Wang, H. Chao, L.N. Ji, A.L. Xu, Synthesis, characterization, and anticancer activity of ruthenium(II)-beta-carboline complex, Eur. J. Med. Chem. 70 (2013) 120–129.
[55] C. Gaiddon, P. Jeannequin, P. Bischoff, M. Pfeffer, C. Sirlin, J.P. Loeffler, Ruthenium (II)-derived organometallic compounds induce cytostatic and cytotoxic effects on mammalian cancer cell lines through p53-dependent and p53-independent mechanisms, J. Pharmacol. Exp. Ther. 315 (3) (2005) 1403–1411.
[56] L. Li, Y.S. Wong, T. Chen, C. Fan, W. Zheng, Ruthenium complexes containing bisbenzimidazole derivatives as a new class of apoptosis inducers, Dalton Trans. 41 (4) (2012) 1138–1141.
[57] Y.-Y. Xie, Z.-Z. Li, G.-J. Lin, H.-L. Huang, X.-Z. Wang, Z.-H. Liang, G.-B. Jiang, Y.-J. Liu, DNA interaction, cytotoxicity, apoptotic activity, cell cycle arrest, reactive oxygen species and mitochondrial membrane potential assay induced by ruthenium (II) polypyridyl complexes, Inorg. Chim. Acta 405 (2013) 228–234.
[58] K. Martin-Hernandez, J.M. Rodriguez-Vargas, V. Schreiber, F. Dantzer, Expanding functions of ADP-ribosylation in the maintenance of genome integrity, Semin. Cell Dev. Biol. 63 (2017) 92–101.
[59] S. Elmore, Apoptosis: a review of programmed cell death, Toxicol. Pathol. 35 (4) (2007) 495–516.
[60] M. Los, M. Mozoluk, D. Ferrari, A. Stepczynska, C. Stroh, A. Renz, Z. Herceg, Z.Q. Wang, K. Schulze-Osthoff, Activation and caspase-mediated inhibition of PARP: a molecular switch between fibroblast necrosis and apoptosis in death receptor signaling, Mol. Biol. Cell 13 (3) (2002) 978–988.
[61] J.D. Amaral, J.M. Xavier, C.J. Steer, C.M.P. Rodrigues, The role of p53 in apoptosis, Discov. Med. 9 (45) (2010) 145–152.
[62] I. Shats, M. Milyavsky, X. Tang, P. Stambolsky, N. Erez, R. Brosh, I. Kogan, I. Braunstein, M. Tzukerman, D. Ginsberg, V. Rotter, p53-dependent down-regulation of telomerase is mediated by p21waf1, J. Biol. Chem. 279 (49) (2004) 50976–50985.
[63] G. He, Z.H. Siddik, Z. Huang, R. Wang, J. Koomen, R. Kobayashi, A.R. Khokhar, J. Kuang, Induction of p21 by p53 following DNA damage inhibits both Cdk4 and Cdk2 activities, Oncogene 24 (18) (2005) 2929–2943.
[64] J.S. Ho, W. Ma, D.Y. Mao, S. Benchimol, p53-Dependent transcriptional repression of c-myc is required for G1 cell cycle arrest, Mol. Cell. Biol. 25 (17) (2005) 7423–7431.
[65] M. Sachdeva, S. Zhu, F. Wu, H. Wu, V. Walia, S. Kumar, R. Elble, K. Watabe, Y.Y. Mo, p53 represses c-Myc through induction of the tumor suppressor miR-145, Proc. Natl. Acad. Sci. U. S. A. 106 (9) (2009) 3207–3212.
[66] J. Stallock, K. Molyneaux, K. Schaible, C.M. Knudson, C. Wylie, The pro-apoptotic gene Bax is required for the death of ectopic primordial germ cells during their migration in the mouse embryo, Development 130 (26) (2003) 6589–6597.
[67] K. Nakano, K.H. Vousden, PUMA, a novel proapoptotic gene, is induced by p53, Mol. Cell 7 (3) (2001) 683–694.
[68] H. Yamaguchi, J. Wyckoff, J. Condeelis, Cell migration in tumors, Curr. Opin. Cell Biol. 17 (5) (2005) 559–564.
[69] Q. Wu, K. Zheng, S. Liao, Y. Ding, Y. Li, W. Mei, Arene ruthenium(II) complexes as low-toxicity inhibitor against the proliferation, migration, and invasion of MDA-MB-231 cells through binding and stabilizing c-myc G-quadruplex DNA, Organometallics 35 (3) (2016) 317–326.
[70] P. Nowak-Sliwinska, J.R. van Beijnum, A. Casini, A.A. Nazarov, G. Wagnieres, H. van den Bergh, P.J. Dyson, A.W. Griffioen, Organometallic ruthenium(II) arene compounds with antiangiogenic activity, J. Med. Chem. 54 (11) (2011) 3895–3902.
[71] Y. Benabdelouahab, L. Munoz-Moreno, M. Frik, I. de la Cueva-Alique, M.A. El Amrani, M. Contel, A.M. Bajo, T. Cuenca, E. Royo, Hydrogen bonding and anticancer properties of water-soluble chiral p-cymene Ru(II) compounds with amino-oxime ligands, Eur. J. Inorg. Chem. 2015 (13) (2015) 2295–2307.